applied sciences

MDPI

Article

Stability Analysis of Filled-Slope Reinforced by Frame with Prestressed Anchor-Plates under Static Action

Jun Zhang [1], Weili Li [2,*] and Shuaihua Ye [1,*]

[1] School of Civil Engineering, Lanzhou University of Technology, Lanzhou 730050, China
[2] GanSu CSCEC Municipal Engineering Investigation And Design Institute Co., Ltd., Lanzhou 730000, China
* Correspondence: csceclwl@163.com (W.L.); yeshuaihua@163.com (S.Y.)

Abstract: Because of the current situation where the stability research of filled-slope reinforced by a frame with prestressed anchor-plates lags behind the actual engineering application, based on the ultimate balance theory, the calculation formulas of stability factor under the four arc slip surface of filled-slopes reinforced by a frame with prestressed anchor-plates are derived by using the improved Bishop method; the corresponding search method of the most dangerous slip surface is given and the calculation formulas of the pullout force of anchor-plates are improved. Based on two examples, the stability results calculated by the proposed algorithm are compared with those calculated by PLAXIS 3D and GeoStudio 2012 finite element software, and the following conclusions are drawn. (1) The improved pullout force of anchor-plates takes into account the friction of the front and rear surface of the anchor-plate and the effect of cohesion of fill soil in the passive earth pressure on the front end of the anchor-plate, which makes the force of the anchor-plate more complete. (2) The stability factor of example 1 calculated by this method differs from the results simulated by PLAXIS 3D and GeoStudio 2012 by 4.6% and 7.1%, respectively; the stability factor of example 2 calculated by this method differs from the results simulated by PLAXIS3D and GeoStudio 2012 by 3.2% and 4.5%, respectively, which can meet the engineering requirements. (3) The stability analysis method of filled-slope reinforced by a frame with prestressed anchor-plates that is proposed is reasonable and suitable for any arc slip surface in the filled-slope reinforced by a frame with prestressed anchor-plates, and it provides some guiding values for the design of practical engineering.

Keywords: filled-slope; static action; frame with prestressed anchor-plates; stability

check for updates

Citation: Zhang, J.; Li, W.; Ye, S. Stability Analysis of Filled-Slope Reinforced by Frame with Prestressed Anchor-Plates under Static Action. *Appl. Sci.* **2023**, *13*, 1615. https://doi.org/10.3390/app13031615

Academic Editor: Bing Bai

Received: 11 December 2022
Revised: 6 January 2023
Accepted: 18 January 2023
Published: 27 January 2023

Copyright: © 2023 by the authors. Licensee MDPI, Basel, Switzerland. This article is an open access article distributed under the terms and conditions of the Creative Commons Attribution (CC BY) license (https://creativecommons.org/licenses/by/4.0/).

1. Introduction

In recent years, a large number of cut slopes and filled-slopes have often been produced in the process of urbanization construction. In order to prevent the occurrence of landslides, appropriate supporting structures must be adopted to reinforce the slopes [1–6]. In the project, gravity retaining walls [7,8], cantilever retaining walls [9,10], counterfort retaining walls [11,12] and anchor slab retaining walls [13,14] are generally used to reinforce filled-slopes. However, when the slope exceeds 15 m, if the above methods are used, the reinforcement effect is not ideal, the construction is difficult and the economy is unreasonable, and then there are some hidden dangers. Technical code for building slope engineering (GB 50330-2013) [15] stipulates that special designs should be carried out for soil slopes above 15 m, and effective and reliable strengthening measures should be taken. To this end, Ye and Zhu [16,17] proposed the frame with prestressed anchor-plates suitable for filled-slopes. This structure not only overcomes the height limitation of the above filled-slope supporting structure, but also has the advantages of convenient construction, low cost, and good overall stability. Plus, the deformation of the filled-slope can be well controlled by applying prestress to the anchor-plates. At present, this structure has been applied to the practical project; Figure 1 is the scene picture of the anchor-plate, and Figure 2 is a filled-slope reinforced by a frame with prestressed anchor-plates.

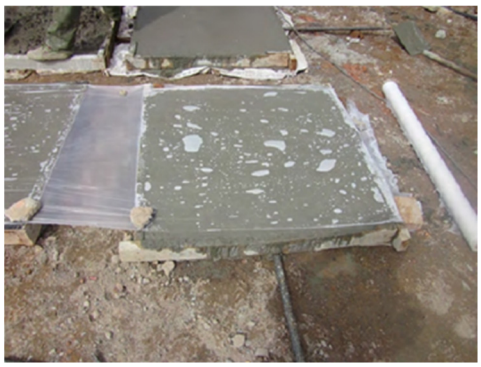


Figure 1. The scene picture of the anchor-plate.

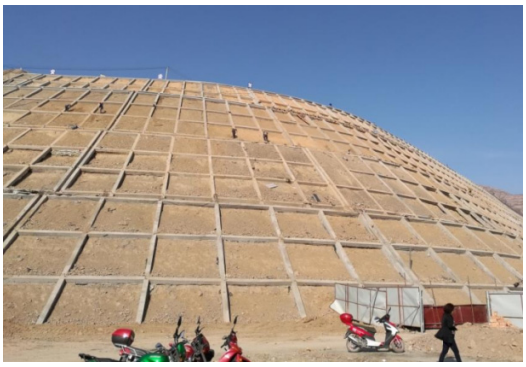


Figure 2. Filled-slope reinforced by a frame with prestressed anchor-plates.

As a new type of flexible supporting structure, the structural form and working mechanism of frames with prestressed anchor-plates are similar to those of frame prestressed anchor supporting structures and anchor slab retaining walls. Under the action of the supporting structure, the soil properties of the original slope will change, and the deformation and interface characteristics of the soil material are different from the original slope, which will have a great impact on the stability of the slope [18–21]. Therefore, the slope stability analysis considering the action of the supporting structure is also the core content in the field of slope research. The current research on the stability of slopes reinforced by a frame prestressed anchor and anchor slab retaining wall under static action are as follows. Li et al. [22] established an intelligent optimization calculation model of anchor tension at each layer that satisfies the excavation process stability and realized the real-time dynamic analysis of stability of slopes reinforced by a frame prestressed anchor in the process of excavation and reinforcement. Zhu et al. [23], based on the basic principle of the upper limit theory of plastic mechanics, the safety coefficient calculation formula of a slope reinforced by a frame with prestressed anchors is derived. He et al. [24] proposed a stability analysis method of a suspended-anchor earth retaining wall. The current research on filled-slopes reinforced by a frame with a prestressed anchor-plate supporting structure are as follows. Ye et al. [16] compared numerical simulation results with the actual monitoring data of a filled-slope reinforced by the frame with prestressed anchor-plates, and found that this supporting structure can effectively improve the stability of the filled-slope and can effectively control the displacement and deformation of the filled-slope. Zhu et al. [25], based on the ultimate balance theory, the stability calculation method of a filled-slope reinforced by a frame with prestressed anchor-plates is proposed by using the circular vertical simple slice method, and the ultimate bearing capacity calculation formula of anchor-plates is given. In addition to the above theoretical research on slope stability with a supporting structure, when using finite element software to analyze the stability of a filled-slope reinforced by a frame with prestressed anchor-plates, the simulation of anchor-plates is also worthy of attention. Phung et al. [26,27] used finite element software to simulate different types

of plates and analyzed the simulation results, which provided a certain reference for the simulation of anchor-plates.

From the present situation of the above research, it can be found that the theoretical research and numerical simulation research on the stability of filled-slopes reinforced by a frame with prestressed anchor-plates is very immature. Thus, this paper proposes four types of slip surfaces that may occur when the frame with prestressed anchor-plates is used to reinforce the filled-slope. It is divided into two types according to whether there is the lowest point F of the slip surface. Based on the ultimate balance theory, the improved Bishop method is used to deduce the stability calculation formula under two different types of slip surfaces, the corresponding search model of the most dangerous slip surface is given, and the calculation theory of pullout force of anchor-plates is improved. The two kinds of stability algorithms are optimized, and the stability analysis flow of a filled-slope reinforced by a frame with a prestressed anchor-plate supporting structure is given, which makes it more applicable. Based two examples, the stability results calculated by the proposed algorithm are compared with those calculated by PLAXIS 3D finite element software and GeoStudio 2012 finite element software to verify the rationality of the proposed stability analysis method of a filled-slope reinforced by a frame with prestressed anchor-plates. This method is suitable for any arc slip surface that appears on the filled-slope reinforced by the frame with prestressed anchor-plates, and it provides some guiding value for the design of practical engineering.

2. Composition and Working Mechanism of Frame with Prestressed Anchor-Plate Supporting Structure

The frame with a prestressed anchor-plate supporting structure is composed of a reinforced concrete frame and an anchor-plate, which belongs to a kind of soft filled-slope supporting structure in the geotechnical anchoring structure system. Its elevation and section drawings are shown in Figures 3 and 4. The anchor-plate consists of a tie rod and a reinforced concrete prefabricated panel. When the filled-slope is reinforced, the structural system is like a floor well-shaped beam structure standing on the soil, the prestressed anchor-plate is anchored in the soil of the slope, and the anchor head of the anchor-plate is connected to the node of the frame beam. The earth pressure on the frame beam is finally transferred to the anchor-plate located in the stable area through the pull rod, and then the slope stability is maintained by the friction between the anchor-plate and the surrounding soil.

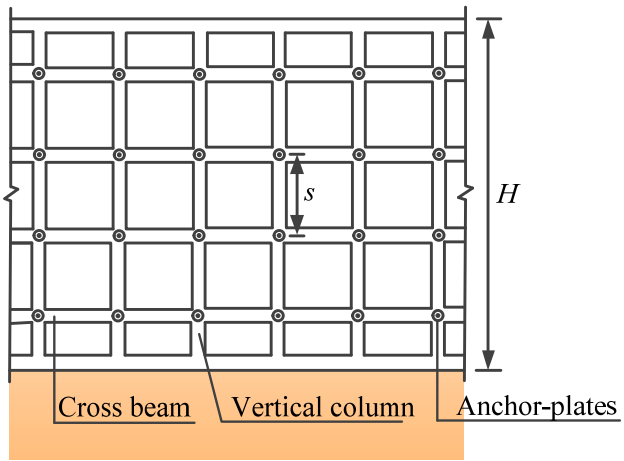


Figure 3. Elevation view of a frame with a prestressed anchor-plate supporting structure.

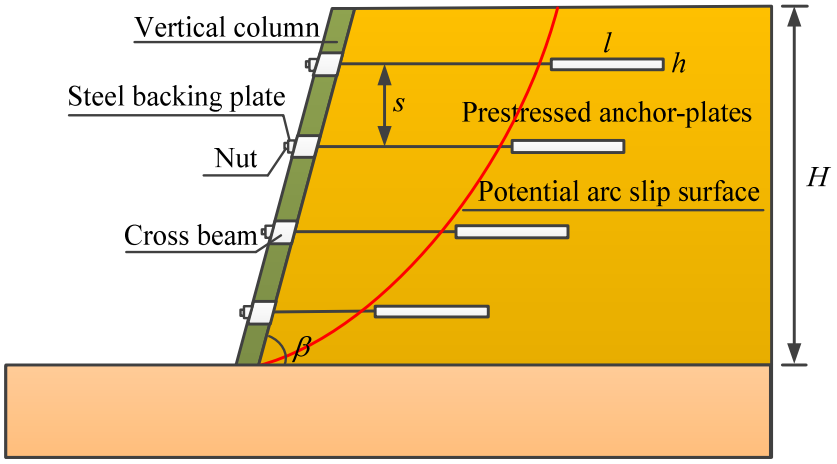


Figure 4. Section view of a frame with a prestressed anchor-plate supporting structure.

3. Types of Slip Surfaces That May Appear in The Reinforcement of The Filled-Slope by the Frame with Prestressed Anchor-Plates

Based on the failure of soil slopes, the filled-slope reinforced by a frame with prestressed anchor-plates may actually appear in the following four types of slip surfaces.

(1) When the arc slip surface passes over the toe of the slope, it is called the slope toe circle [28,29]. There are two main forms of slope toe circle, one of which is shown in Figure 5. The angle between the tangent of any point on the slip plane and the horizontal direction is between 0°~90°, and the center *P* of the slip plane is located at the upper left of the whole slope. There is much research on slope stability in the case of this type of slip surface.

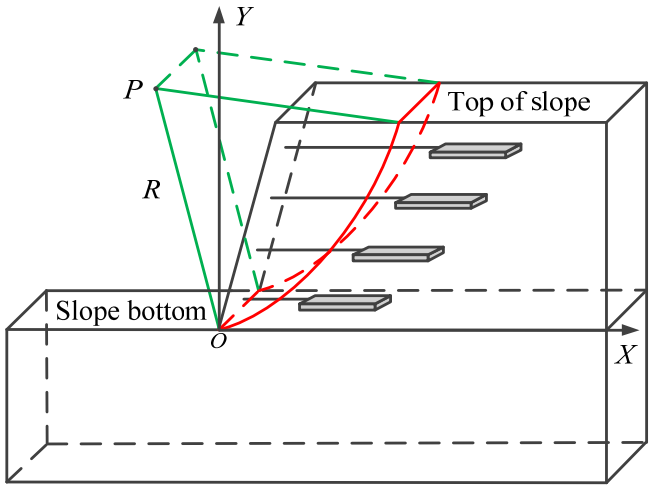


Figure 5. Schematic diagram of slope toe circle 1.

(2) Another form of the slope toe circle is shown in Figure 6. Although this slip surface passes over the toe of the slope, the angle between the tangent and the horizontal direction at the toe of the slope is a negative angle, and the lowest point *F* on the arc slip surface is on the right side of the toe of the slope.

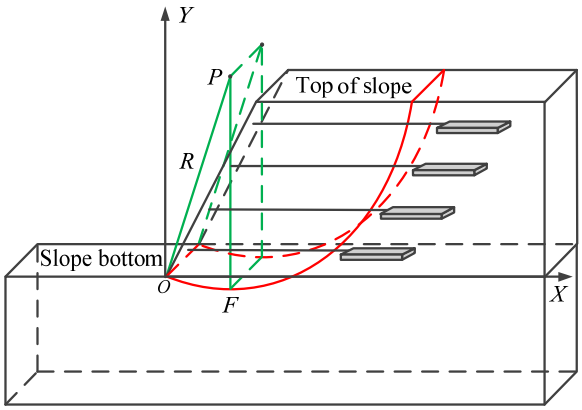


Figure 6. Schematic diagram of slope toe circle 2.

(3) When the arc slip surface passes through a certain position other than the toe of the slope, it is called the midpoint circle [28,29]. There are also two main forms of midpoint circles, one of which is shown in Figure 7. The lowest point *F* and the center *P* of the arc slip surface are both located on the right side of the toe of the slope.

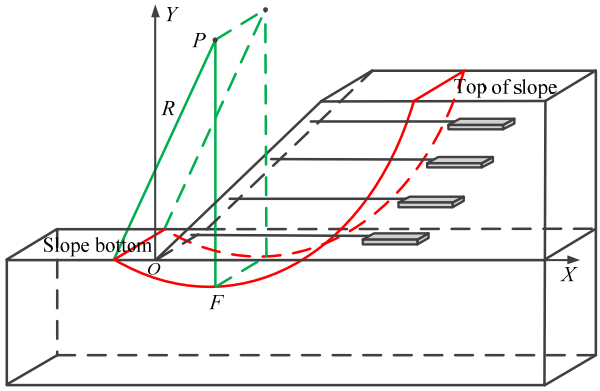


Figure 7. Schematic diagram of slope toe circle 2.

(4) Another form of the midpoint circle is shown in Figure 8. The lowest point *F* and center *P* of the arc slip surface are located on the left side of the toe of the slope, and the sliding range of this slip surface is larger than that shown in Figure 7.

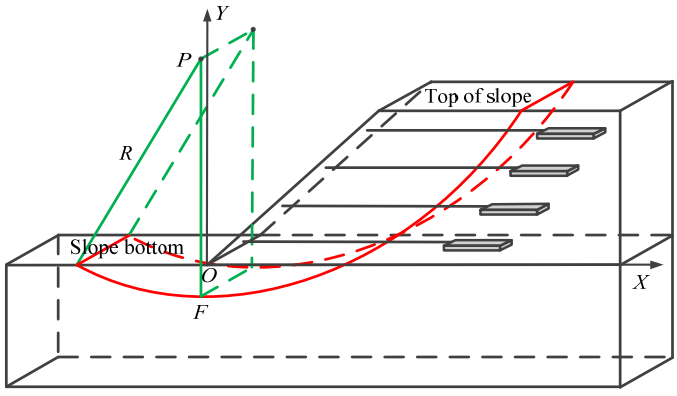


Figure 8. Schematic diagram of midpoint circle 1.

Among the four types of slip surfaces mentioned above, they are divided into two types according to whether there is the lowest point *F*. The slope toe circle 1 is classified as the first type slip surface, and the slope toe circle 2, the midpoint circle 1 and the midpoint circle 2 are classified as the second type slip surface.

4. Stability Analysis Model of Filled-Slope Reinforced by Frame with Prestressed Anchor-Plates

The simplified Bishop method, as one of the ultimate balance methods, is considered to be a "non-strict" method because it ignores the shear force between strips and does not strictly satisfy the equilibrium conditions. However, many scholars have found that the stability factors of slopes obtained by the improved Bishop method and the strict method are very close, which can be called the strict strip method [30–32]. The traditional simplified Bishop method is only suitable for the stability analysis of natural slope, but cannot be directly used to analyze the stability of a slope with a supporting structure. Therefore, considering the influence of a frame with a prestressed anchor-plate supporting structure on the stability of a filled-slope, this paper improves the traditional simplified Bishop method and deduces the stability calculation formula which is suitable for a filled-slope reinforced by a frame with prestressed anchor-plates.

4.1. Basic Assumptions

According to the central idea of the Bishop method, the following assumptions are made [30]:

(1) The slope is a soil slope, and the slip surface is an arc slip surface.
(2) The shear strength of slope soil obeys Mohr–Coulomb criterion.
(3) The inter-strip shear force is ignored, and the inter-strip horizontal force is considered.
(4) The effect of the anchor-plate on the slope is equivalent to the force perpendicular to the tangent direction of the slip plane, and this force is uniformly distributed on the slip surface.

4.2. Stability Analysis in the Case of the First Type of Slip Surface

4.2.1. Solving the Stability Factor

The diagram of the stability analysis for the first type of slip surface is shown in Figure 9.

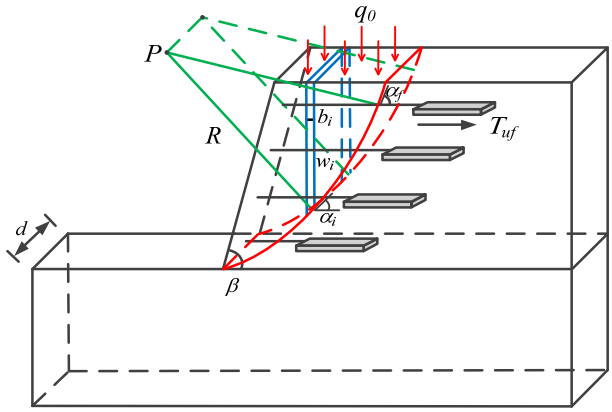


Figure 9. Diagram of stability analysis for the first type of slip surface.

When analyzing the stability of the slope shown in Figure 9 based on the simplified Bishop method, due to the supporting effect of the frame with prestressed anchor-plates on the slope, the force of the soil strip is different from that of the soil strip without reinforcement. Thus, the resistant shear force provided by the anchor-plates and the resistant shear force of the soil itself cannot be simply superimposed. As shown in Figure 10, T_u' and T_u'' can be obtained by decomposing the ultimate bearing capacity provided by anchor-plates. T_u' and soil have the same direction of resistant shear force of the soil, which directly provides resistant shear force for the sliding body. T_u'' is perpendicular to T_u', and it provides resistant shear force for the sliding body through friction with the soil outside the sliding surface. In order to derive the formula for calculating the slope stability under the action of the supporting structure, T_u' is equivalent to the force in the same direction

as T_u'' according to Equation (2). The force provided by the anchor-plates is uniformly distributed on the slip surface as the force perpendicular to the tangent direction of the slip surface, so the force provided by the anchor-plates on the soil strip i is as follows:

$$N_{ui} = [\sum_{f=1}^{t} (T_{uf} \sin \alpha_f + T_{uf} \cos \alpha_f F_s / \tan \varphi_f)] b_i \sec \alpha_i / L \quad (1)$$

where t is the total number of layers of the prestressed anchor-plate; T_{uf} is the ultimate bearing capacity of the f-layer anchor-plate, which can be determined by Equation (31); α_f is the angle between the tangent line and the horizontal direction at the intersection of the f-layer anchor-plate and the slip surface; φ_f is the internal friction angle of the soil at the intersection point of the f-layer anchor-plate and the slip surface; L is the total arc length of the slip surface.

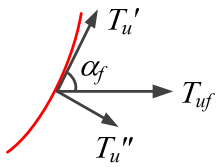


Figure 10. Resolution diagram of the ultimate bearing capacity of the anchor-plate.

The force diagram of the soil strip considering the action of the supporting structure is shown in Figure 11, according to the Mohr–Coulomb criterion [30]:

$$T_i d = N_i d \tan \varphi_i / F_s + c_i b_i d \sec \alpha_i / F_s \quad (2)$$

where F_s is the stability factor of slope; $T_i d$ is the shear force at the bottom of the soil strip i; $N_i d$ is the normal force at the bottom of the soil strip i; α_i is the angle between the tangent line and the horizontal direction at the slip surface of the soil strip i; c_i is the cohesion at the slip surface of the soil strip i; φ_i is the angle of internal friction at the slip surface of the soil strip i; b_i is the width of the soil strip i; d is the thickness of sliding element.

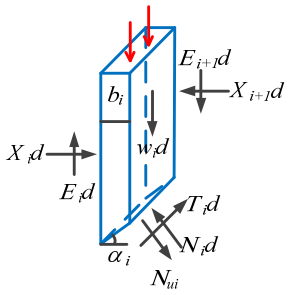


Figure 11. Force diagram of soil strip i.

Considering the vertical force balance [30]:

$$(N_i d - N_{ui}) \cos \alpha_i + T_i d \sin \alpha_i = (W_i + q_0 b_i) d \quad (3)$$

where $W_i d$ is the dead weight of the soil strip i; q_0 is the uniformly distributed load on the top of the slope.

Simultaneous Equations (2) and (3) can be obtained:

$$N_i d = [(W_i + q_0 b_i) d + N_{ui} \cos \alpha_i - c_i b_i d \tan \alpha_i / F_s] / m_{\alpha i} \quad (4)$$

$$T_i d = [(W_i + q_0 b_i) d \tan \varphi_i / F_s + N_{ui} \cos \alpha_i \tan \varphi_i / F_s + c_i b_i d / F_s] / m_{\alpha i} \quad (5)$$

$$m_{\alpha i} = \cos \alpha_i + \sin \alpha_i \tan \varphi_i / F_s \quad (6)$$

Consider the moment balance to the center of the circle:

$$\sum_{i=1}^{n} T_i dR = \sum_{i=1}^{n} (W_i + q_0 b_i) d \sin \alpha_i R \tag{7}$$

where n is the number of the strips of sliding body; R is the arc radius of the slip surface.

Substitute Equation (5) into Equation (7) to obtain:

$$F_s = \frac{\sum_{i=1}^{n} [(W_i + q_0 b_i) d \tan \varphi_i + c_i b_i d + N_{ui} \cos \alpha_i \tan \varphi_i] R / m_{\alpha i}}{\sum_{i=1}^{n} (W_i + q_0 b_i) d \sin \alpha_i R} \tag{8}$$

Substitute Equation (1) into Equation (8) to obtain:

$$F_s = \frac{\sum_{i=1}^{n} [(W_i + q_0 b_i) d \tan \varphi_i + c_i b_i d + \sum_{f=1}^{t} (T_{uf} \sin \alpha_f + T_{uf} \cos \alpha_f F_s / \tan \varphi_f) b_i \tan \varphi_i / L] R / m_{\alpha i}}{\sum_{i=1}^{n} (W_i + q_0 b_i) d \sin \alpha_i R} \tag{9}$$

4.2.2. Search for Models of Slip Surfaces

(1) The center coordinates and radius of the slip surface

The search model of the first kind of slip surface is shown in Figure 12. Although the established model is a three-dimensional model, the slip surface always changes in the *xoy* plane, so it is simplified to two-dimensional coordinates. In the Cartesian coordinate system, $P(x_c, y_c)$, $C(e, H)$, $O(0, 0)$, the angle between the tangent of point O and the horizontal is θ, the slope of the tangent is k', $k' = tan\theta$.

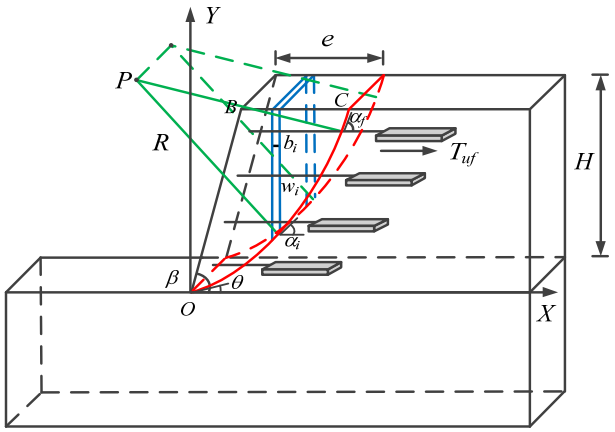


Figure 12. Search model of the first kind of slip surface.

Then the slip surface equation is:

$$(x - x_c)^2 + (y - y_c)^2 = R^2 \tag{10}$$

And satisfies:

$$\left.\begin{array}{l} {x_c}^2 + {y_c}^2 = R^2 \\ (e - x_c)^2 + (H - y_c)^2 = R^2 \\ x_c = -k' y_c \end{array}\right\} \tag{11}$$

Combining Equations (10) and (11) yields:

$$\left.\begin{array}{l} x_c = \frac{-k'(H^2+e^2)}{2H-2k'e} \\ y_c = \frac{H^2+e^2}{2H-2k'e} \\ R = \frac{\sqrt{1+k'^2}(H^2+e^2)}{2H-2k'e} \end{array}\right\} \tag{12}$$

Therefore, the slip surface is controlled by θ and e. The value range of θ and e is determined, and the appropriate step size is set respectively, and the search of slip surface can be realized by constantly changing.

(2) The angle between the tangent of any point on the arc and the horizontal plane

At any point $M(x_k, y_k)$ on the arc, the angle between the tangent and the horizontal plane is α_k, which can be obtained from the geometric relationship:

$$\sin \alpha_k = \frac{x_c - x_k}{R} \tag{13}$$

$$\cos \alpha_k = \frac{y_c - y_k}{R} \tag{14}$$

(3) The self-weight of the soil block i

According to Figure 9, the coordinate of the soil strip i at the slip surface is (x_i,y_i), and when the upper end of the soil strip is on OB, the upper coordinate is (x_{i1},y_{i1}), so the formula for calculating the self-weight of the soil strip i is as follows:

$$W_i = \begin{cases} \gamma b_i (H - y_i) \; x_i \geq \frac{H}{\tan \beta} \\ \gamma b_i (y_{i1} - y_i) \; 0 \leq x_i \leq \frac{H}{\tan \beta} \end{cases} \tag{15}$$

where γ is the weight of fill soil.

4.3. Stability Analysis in the Case of the Second Type of Slip Surface

4.3.1. Solving the Stability Factor

The diagram of the stability analysis for the second type of slip surface and the force diagram of soil strip j are shown in Figures 13 and 14.

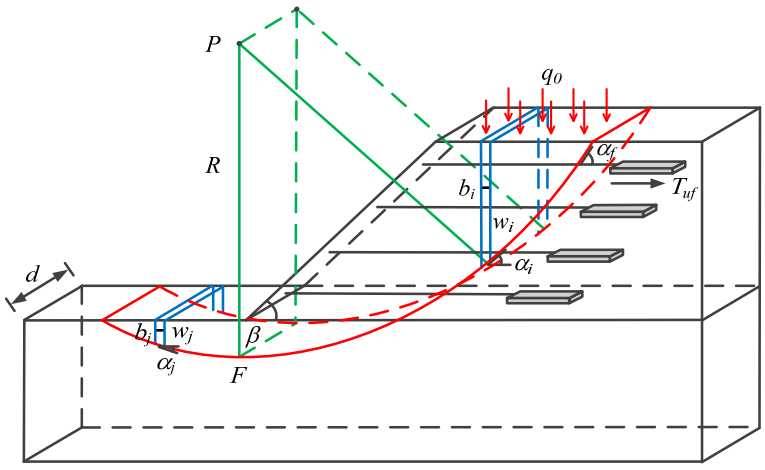


Figure 13. Diagram of stability analysis for the second type of slip surface.

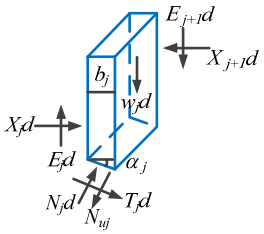


Figure 14. Force diagram of soil strip *j*.

Soil strip on the left side of *OF*.

The force provided by the anchor-plates on the soil strip *j* is as follows:

$$N_{uj} = [\sum_{f=1}^{t} (T_{uf} \sin \alpha_f + T_{uf} \cos \alpha_f F_s / \tan \varphi_f)] b_j \sec \alpha_j / L \tag{16}$$

By Mohr–Coulomb criterion [30]:

$$T_j d = N_j d \tan \varphi_j / F_s + c_j b_j d \sec \alpha_j / F_s \tag{17}$$

where T_jd is the shear force at the bottom of the soil strip *j* at the left on point *F*; N_jd is the normal force at the bottom of the soil strip *j* at the left on point *F*; b_j is the width of the soil strip *j* at the left on point *F*; c_j is the cohesion at the slip surface of the soil strip *j* at the left on point *F*; φ_j is the angle of internal friction at the slip surface of the soil strip *j* at the left on point *F*; α_j is the angle between the tangent line and the horizontal plane at the slip plane of the soil strip *j* at the left on point *F*.

Consider the vertical force balance [30]:

$$(N_j d - N_{uj}) \cos \alpha_j - T_j d \sin \alpha_j = W_j d \tag{18}$$

where W_jd is the dead weight of the soil strip *j* at the left on point *F*.

Simultaneous Equations (17) and (18) can be obtained:

$$N_j d = (W_j d + N_{uj} \cos \alpha_j + c_j b_j \tan \alpha_j / F_s) / m_{\alpha j} \tag{19}$$

$$T_j d = (W_j d \tan \varphi_j / F_s + N_{uj} \cos \alpha_j \tan \varphi_j / F_s + c_j b_j d / F_s) / m_{\alpha j} \tag{20}$$

$$m_{\alpha j} = \cos \alpha_j - \sin \alpha_j \tan \varphi_j / F_s \tag{21}$$

Soil strip on the right side of *OF*.

The force analysis of the soil strip on the right side of *OF* is similar to that in the case of slip surface 1, and the final deduced results are Equations (4)–(6).

Consider the moment balance to the center of the circle:

$$\sum_{i=1}^{n} T_i d R + \sum_{j=1}^{m} T_j d R = \sum_{i=1}^{n} (W_i + q_0 b_i) d \sin \alpha_i R - \sum_{j=1}^{m} W_j d \sin \alpha_j R \tag{22}$$

where *n* is the number of the strips of sliding body at the right on point *F*; *m* is the number of the strips of sliding body at the left on point *F*; *R* is the arc radius of the slip surface; T_id is the shear force at the bottom of the soil strip *i* at the right on point *F*; W_id is the dead weight of the soil strip *i* at the right on point *F*; α_i is the angle between the tangent line and the horizontal plane at the slip surface of the soil strip *i* at the right on point *F*.

Substitute Equations (5) and (20) into Equation (22) to obtain:

$$F_s = \frac{\sum_{i=1}^{n}[(W_i + q_0 b_i)d\tan\varphi_i + c_i b_i d + N_{ui}\cos\alpha_i \tan\varphi_i]R/m_{\alpha i} + \sum_{j=1}^{m}[(W_j d\tan\varphi_j + c_j b_j d + N_{uj}\cos\alpha_j \tan\varphi_j]R/m_{\alpha j}}{\sum_{i=1}^{n}(W_i + q_0 b_i)d\sin\alpha_i R - \sum_{j=1}^{m} W_j d\sin\alpha_j R} \quad (23)$$

where b_i = the width of the soil strip i at the right on point F; c_i = the cohesion at the slip surface of the soil strip i at the right on point F; φ_i = the angle of internal friction at the slip surface of the soil strip i at the right on point F.

Substitute Equations (1) and (16) into Equation (23) to obtain:

$$F_s = \frac{\sum_{i=1}^{n}[(W_i + q_0 b_i)d\tan\varphi_i + c_i b_i d + \sum_{f=1}^{t}(T_{uf}\sin\alpha_f + T_{uf}\cos\alpha_f F_s/\tan\varphi_f)b_i\tan\varphi_i/L]R/m_{\alpha i} + \sum_{j=1}^{m}[W_j d\tan\varphi_j + c_j b_j d + \sum_{f=1}^{t}(T_{uf}\sin\alpha_f + T_{uf}\cos\alpha_f F_s/\tan\varphi_f)b_j\tan\varphi_j/L])R/m_{\alpha j}}{\sum_{i=1}^{n}(W_i + q_0 b_i)d\sin\alpha_i R - \sum_{j=1}^{m} W_j d\sin\alpha_j R} \quad (24)$$

4.3.2. Search for Models of Slip Surfaces

(1) The center coordinates and radius of the slip surface

The search model of the second kind of slip surface is shown in Figure 15. Since the slip surface always changes in the *xoy* plane, it is simplified to two-dimensional coordinates. In the Cartesian coordinate system, $P(x_c, y_c)$, $C(e, H)$, $A(-e_0, 0)$, $O(0, 0)$, the angle between the tangent of point A and the horizontal is θ, and the slope of the tangent is k', $k' = -tan\theta$.

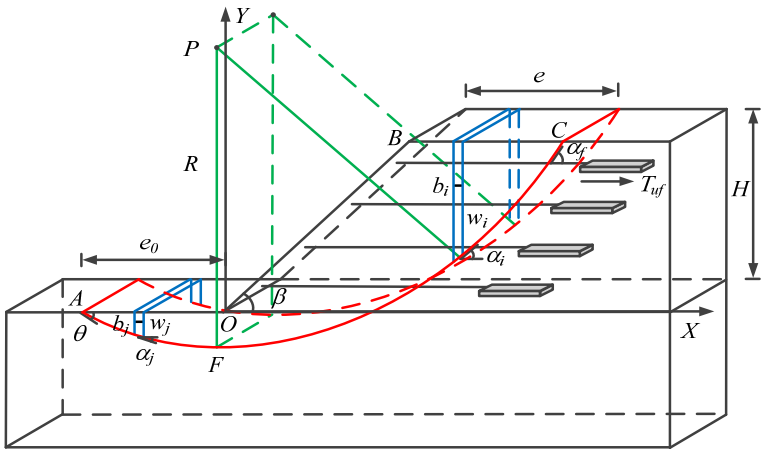


Figure 15. Search model of the second kind of slip surface.

Then the slip surface equation is:

$$(x - x_c)^2 + (y - y_c)^2 = R^2 \quad (25)$$

And satisfies:

$$\left.\begin{array}{l}(-e_0 - x_c)^2 + {y_c}^2 = R^2 \\ (e - x_c)^2 + (H - y_c)^2 = R^2 \\ x_c = -(k' y_c + e_0)\end{array}\right\} \quad (26)$$

Combining Equations (25) and (26) yields:

$$\left.\begin{array}{l} x_c = -e_0 - \frac{k'[(e+e_0)^2+H^2]}{2H-2k'(e+e_0)} \\ y_c = \frac{(e+e_0)^2+H^2}{2H-2k'(e+e_0)} \\ R = \frac{\sqrt{1+k'^2}[(e+e_0)^2+H^2]}{2H-2k'(e+e_0)} \end{array}\right\} \quad (27)$$

Therefore, the slip surface is controlled by θ, e_0 and e. The value range of θ, e_0 and e is determined, and the appropriate step size is set respectively, and the search of slip surface can be realized by constantly changing.

(2) The angle between the tangent of any point on the arc and the horizontal plane

At any point $M'(x_k, y_k)$ on the arc, the angle between the tangent and the horizontal plane is α_k, which can be obtained from the geometric relationship:

$$\sin\alpha_k = \frac{|x_c - x_k|}{R} \quad (28)$$

$$\cos\alpha_k = \frac{y_c - y_k}{R} \quad (29)$$

(3) The self-weight of the soil block i and j

It can be seen from Figure 12 that the calculation of the self-weight of the soil strip under the second type of slip surface is more complicated. The coordinates of the soil strip i at the slip surface are (x_i, y_i). When the upper end of the soil strip i is on the OB, its upper coordinate is (x_{i1}, y_{i1}). The coordinates of the soil strip j at the slip plane are (x_j, y_j). When the upper end of the soil strip j is on OB, its upper coordinate is (x_{j1}, y_{j1}). When the abscissa of the zero-boundary point of the slip surface crossing from the filling layer to the foundation soil layer is x_0, the calculation formulas of the self-weight of the soil strip i and j are as follows:

$$W_{i/j} = \begin{cases} \gamma_1 b_i(H - y_i) & x_i \geq \frac{H}{\tan\beta} \\ \gamma_1 b_i(y_{i1} - y_i) & x_0 \leq x_i < \frac{H}{\tan\beta} \\ \gamma_1 b_i y_{i1} - \gamma_2 b_i y_i & 0 \leq x_i < x_0 \\ -\gamma_2 b_i y_i & x_c \leq x_i < 0 \\ -\gamma_2 b_j y_j & -e_0 \leq x_j < x_c \end{cases} \quad (30)$$

where γ_1 is the weight of fill soil; γ_2 is the weight of foundation soil.

4.4. The Ultimate Bearing Capacity of the Anchor-Plate

For the calculation of the ultimate bearing capacity of the anchor-plate, on the basis of the method in Zhu [25], the calculation method of the pullout resistance of the anchor-plate is improved. The force diagram of the anchor-plate is shown in Figure 16.

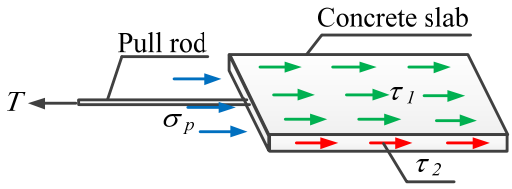


Figure 16. Force diagram of the anchor-plate.

According to Zhu [25], the formula for calculating the pullout force of the anchor-plate is as follows:

$$T_{uf} = \sum \min\{T_s, T_p\} \quad (31)$$

where T_{uf} is the ultimate bearing capacity of the f-layer anchor-plate; T_s is the ultimate tensile force of the steel rod; T_p is the limit value of the pullout force that the anchor-plate can provide, which is composed of the friction resistance of the interface between the anchor-plate and soil and the passive earth pressure of the anchor-plate.

$$T_s = f_y A_s \tag{32}$$

where f_y is the yield strength of the steel rod; A_s is the cross-sectional area of the steel rod.

$$T_p = F_f + Q \tag{33}$$

where F_f is the friction resistance on the anchor-plate; Q is passive earth pressure on the anchor-plate.

Because Zhu [25] did not consider the friction between the two sides of the anchor-plate and the soil when calculating the friction between the anchor-plate and the soil, this paper improves it, and the improved formula for calculating the friction between the anchor-plate and the soil is as follows:

$$F_f = 2(\tau_1 A_1 + \tau_2 A_2) \tag{34}$$

where τ_1 is the shear strength of the interface between the upper and lower interface of the anchor-plate and the soil; τ_2 is the shear strength of the interface between the front and rear interface of the anchor-plate and the soil; A_1 is the upper surface area of anchor-plate; A_2 is the side surface area of anchor-plate:

$$\left.\begin{array}{l} \tau_1 = \mu(\gamma h_0 + q_0) \\ \tau_2 = k_0 \mu(\gamma h_0 + q_0) \end{array}\right\} \tag{35}$$

where γ is the weight of the soil layer where the anchor-plate is located; h_0 is the height from the top of the slope to the soil layer where the anchor-plate is located; q_0 is the uniformly distributed load on the top of the slope; μ is the coefficient of lateral earth pressure:

$$Q = \sigma_p A_3 \tag{36}$$

where σ_p is the passive earth pressure of the soil layer where the anchor-plate is located; A_3 is the front-end area of anchor-plate:

$$\left.\begin{array}{l} A_1 = lb \\ A_2 = lh \\ A_3 = bh \end{array}\right\} \tag{37}$$

where l is the length of the anchor-plate; b = the width of the anchor-plate; h is the height of the anchor-plate.

Because Zhu [25] did not consider the cohesion of the fill soil when calculating the passive earth pressure on the front end of the anchor-plate, which obviously does not conform to the actual engineering situation, the improved formula is as follows:

$$\sigma_p = k_p(\gamma h_0 + q_0) + 2c\sqrt{k_p} \tag{38}$$

where c is the soil cohesion of the soil layer where the anchor-plate is located; k_p is the Rankine passive earth pressure coefficient of the soil around the anchor-plate.

4.5. Stability Analysis Process

Although this paper proposes four forms of slip surface for the reinforcement of a filled-slope with frame prestressed anchor-plates, it is also clear that the form of slip surface is related to the height of the slope, the degree of the slope, and soil conditions of the fill

soil and the foundation soil. However, it is difficult to give clear certain conditions for the occurrence of various slip surfaces; as a result, it is not known which type of slip surface stability analysis process to select when an example is given. Therefore, the stability analysis process under the two types of slip surfaces mentioned above is optimized. The specific analysis process of the stability of the filled-slope reinforced by the frame prestressed anchor-plates is shown in Figure 17.

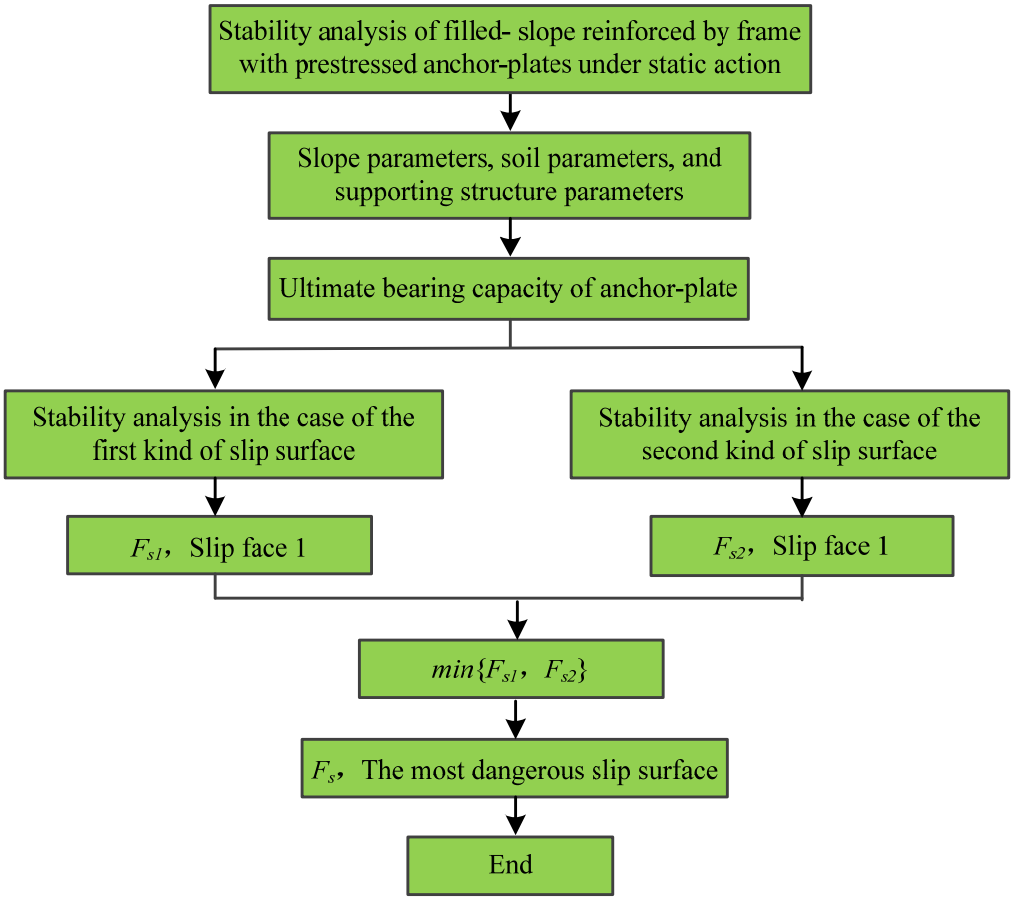


Figure 17. Flow chart of stability analysis.

5. Example Analysis

5.1. Example 1

The specific parameters of the filled-slope reinforced by the frame with prestressed anchor-plates in Lanzhou are as follows. The height of the slope is 12 m, the slope rate is 1: 0.5, the top load of the slope is q_0 = 20 kN/m^2, and the soil parameters are shown in Table 1. The horizontal spacing of the anchor-plate is 3 m, and the length, width and height of the anchor-plate are 4 m, 1 m, and 0.1 m, respectively, and the parameters of anchor-plates for each layer are shown in Table 2.

Table 1. Soil parameters of example 1.

Soil Layer Name	Natural Heavy γ/(kN/m^3)	Cohesive Force c/(kPa)	Angle of Internal Friction φ/(°)	Elastic Modulus E/(kN/m^2)	Friction Coefficient μ
Fill soil	17	20	24	35,000	0.4
Foundation soil	22	28	34	50,000	

Table 2. Parameters of anchor-plate of example 1.

Layer Number	Relative Ground Height/m	Length of Steel Tie Rod/m	Prestress Value/kN
Fourth floor	10.5	12.5	60
Third floor	7.5	11.0	90
Second floor	4.5	9.5	120
First floor	1.5	8.0	150

5.1.1. Analysis of Pullout Resistance of Anchor-Plate

The pullout force calculation method of anchor-plates in Zhu [25] and the improved method in this paper are used to calculate the pullout force of anchor-plates in example 1, and the results are shown in Table 3.

Table 3. Calculation results of pullout force of anchor-plate in example 1.

Layer Number	Original Method/kN	The Method of This Paper/kN	Percentage of Difference
Fourth floor	151.64	168.81	11.32%
Third floor	326.94	351.12	7.40%
Second floor	502.23	533.43	6.21%
First floor	677.52	715.74	6.08%

It can be seen from Table 3 that the pullout force of the anchor-plate calculated by this method is larger than that calculated by the method in Zhu [25]. This is because this method improves the method in Zhu [25]. From Equation (31) it can be seen that the pullout force of the anchor-plate is composed of the friction between the anchor-plate and the soil and the passive earth pressure on the front end of the anchor-plate, so the improvement of the calculation method of the pullout force of the anchor-plate in Zhu [25] is mainly reflected in two aspects. (1) When calculating the friction resistance between the anchor-plate and the surrounding soil, the friction resistance on the front and rear surface of the anchor-plate is considered in addition to the friction resistance on the upper and lower surface of the anchor-plate. Although the friction force on the front and rear surface of the anchor-plate is much smaller than that on the upper and lower surface, taking it into account will make the force of the anchor-plate more complete. (2) When calculating the passive earth pressure on the front end of the anchor-plate, the effect of soil cohesion is taken into account, which makes the calculation of the pullout force of the anchor-plate more suitable for practical engineering.

5.1.2. Stability Analysis

The stability calculation method of this paper, strength reduction method and ultimate balance method are used to calculate the stability of example 1, respectively.

(1) The method of this paper

The stability of example 1 is calculated by using the stability analysis process in this paper, and the calculated results are shown in Figure 18. It can be clearly seen from Figure 18 that the most dangerous slip surface passes over the toe of the slope, which belongs to the sliding mode of toe circle 1. The position of the most dangerous slip surface is 7 m away from point *B* at the top of the slope, and the calculated stability factor is 1.710.

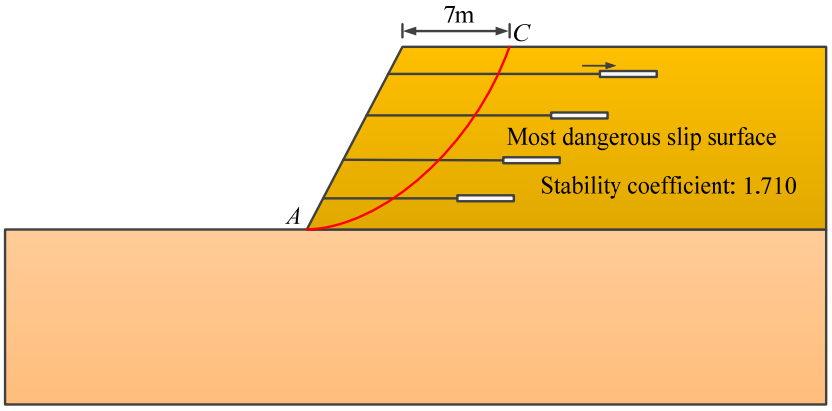


Figure 18. Example 1 calculation results of the stability of this method.

(2) Strength reduction method

PLAXIS 3D finite element software can establish a three-dimensional slope model and calculate its stability, so PLAXIS 3D finite element software is used to calculate the stability of example 1. The anchor-plate is simulated by a large area rectangular beam in the "Embedded beam" element, the frame beam is simulated by the "Beam" element, and the tension bar is simulated by the "Node to node anchor" element. The established three-dimensional model of the filled-slope with a slope ratio of 1:0.5 reinforced by the frame with prestressed anchor-plates is shown in Figure 19.

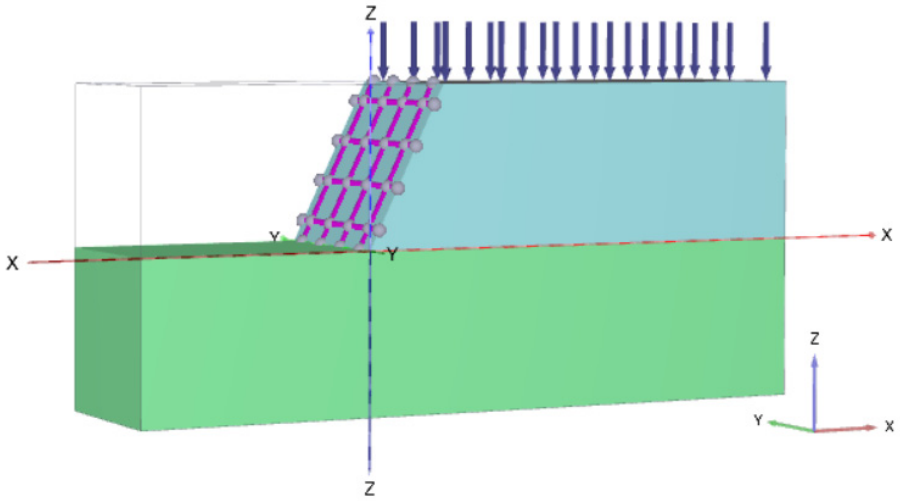


Figure 19. The 1:0.5 model of filled-slope reinforced by a frame with prestressed anchor-plates.

Figure 20 shows the total displacement increment cloud map after the calculation of the model, which can reveal the possible failure mechanism. From Figure 20, it can be clearly seen that the slope failure is an arc sliding failure, and the slip surface will pass over the foot of the slope. Failure may occur in the deformation area of the slope, but the location of the most dangerous slip surface cannot be clearly known. The calculated stability factor is 1.790.

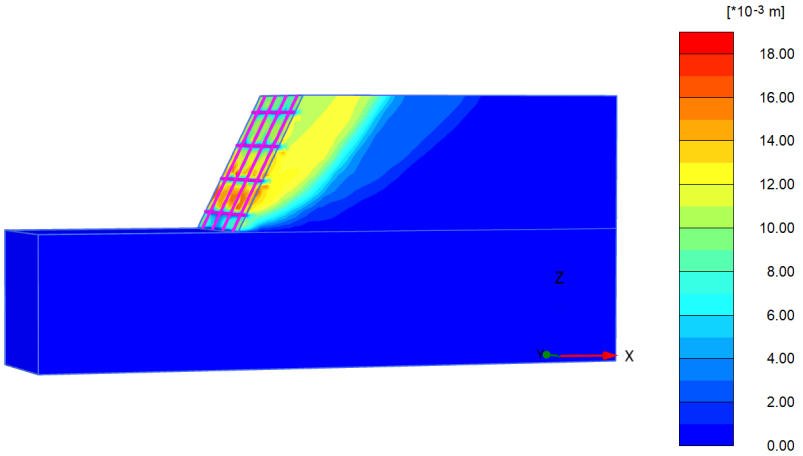


Figure 20. Total displacement increment cloud map of 1:0.5 model.

(3) Ultimate balance method

The slope stability results simulated by PLAXIS 3D are very close to those calculated by this algorithm, but it is not very convincing to verify the rationality of the algorithm in this paper by only relying on the stability results of a slope simulated by a finite element software. Thus, the Bishop method in the SLOPE module of GeoStudio 2012 finite element software is used to calculate the stability of example 1. The anchor-plate is simulated by the "anchor" unit, the specific calculation results are shown in Figure 21. From Figure 21, it can be seen that the most dangerous slip surface passes through the toe of the slope, and the starting point of the slip surface is 6.5 m away from the starting point of the top of slope. The stability factor is 1.840.

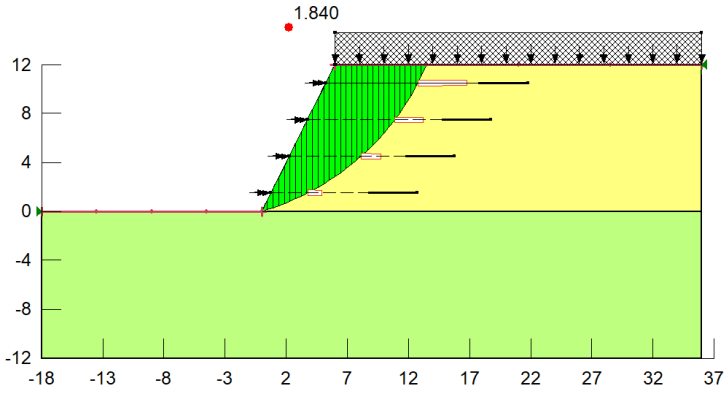


Figure 21. Example 1 calculation results of the stability of Geo.

(4) Comparative analysis

By using the above three methods to calculate the stability of example 1, it is not difficult to see that the slip surfaces obtained by the three methods all pass over the toe of the slope. The stability factor calculated by Geo is the largest, the stability factor calculated by PLAXIS 3D is the second, and the stability factor calculated by this algorithm is the smallest. The stability factor calculated by this method, respectively, differs from the results simulated by Geo and PLAXIS 3D finite element software by 7.1% and 4.6%. By comparing Figure 18 with Figure 21, it can be seen that the position of the most dangerous slip surface obtained by this algorithm is close to that obtained by Geo. Although the location of the most dangerous slip surface cannot be directly obtained in Figure 20, the possible shape of the slip surface can also be seen from the range of areas that may be damaged. The shape of the slip surface reflected in Figure 20 is similar to that of the most dangerous slip surface in Figures 18 and 21, which fully shows that the slip surface search method in this paper

is reliable. The stability factor of this algorithm is smaller than that of two finite element software, which also shows that this algorithm has a certain security reserve.

5.2. Example 2

The specific parameters of the filled-slope reinforced by a frame with prestressed anchor-plates in Longnan are as follows. The height of the slope is 12 m, the slope rate is 1:1, the top load of the slope is q_0 = 20 kN/m^2, and the soil parameters are shown in Table 4. The horizontal spacing of the anchor-plate is 3 m, and the length, width, and height of the anchor-plate are 3 m, 1 m, and 0.1 m, respectively, and the parameters of anchor-plate for each layer are shown in Table 5.

Table 4. Soil parameters of example 2.

Soil Layer Name	Natural Heavy γ/(kN/m^3)	Cohesive Force c/(kPa)	Angle of Internal Friction φ/(°)	Elastic Modulus E/ kN/m^2)	Friction Coefficient μ
Fill soil	17.5	20	22	30,000	0.35
Foundation soil	21	12	30	45,000	

Table 5. Parameters of anchor-plate of example 2.

Layer Number	Relative Ground Height/m	Length of Steel Tie Rod/m	Prestress Value/kN
Fourth floor	10.5	13.5	50
Third floor	7.5	12.5	80
Second floor	4.5	11.5	110
First floor	1.5	10.5	140

5.2.1. Analysis of Pullout Resistance of Anchor-Plate

The pullout force calculation method of anchor-plates in Zhu [25] and the improved method in this paper are used to calculate the pullout force of anchor-plates in example 2, and the results are shown in Table 6.

Table 6. Calculation results of pullout force of anchor-plates in example 2.

Layer Number	Original Method/kN	The Method of This Paper/kN	Percentage of Difference
Fourth floor	102.89	113.00	9.82%
Third floor	224.08	239.53	6.61%
Second floor	346.47	366.06	5.65%
First floor	408.26	492.59	5.20%

It can be seen from Table 6 that the pullout force of the anchor-plates calculated by this method is larger than that calculated by the method of Zhu [25], and the specific reason has been analyzed in example 1. From Equations (31)–(37), it can be seen that the pullout force of the anchor-plate is not only closely related to its own size, but also related to its position. The thicker the soil layer on the anchor-plate is, the greater the friction resistance of the anchor-plate is, and the greater the pullout resistance is, which is the reason for the greater prestress applied to the anchor-plate near the toe of the slope.

5.2.2. Stability Analysis

Like example 1, the stability calculation method of this paper, strength reduction method and ultimate balance method are used to calculate the stability of example 2, respectively.

(1) The method of this paper

The stability of example 2 is calculated by using the stability analysis process in this paper, and the calculated results are shown in Figure 22. It can be clearly seen from Figure 22

that the most dangerous slip surface is far from the foot of the slope, which belongs to the sliding mode of midpoint circle 1. The position of the most dangerous slip surface is 8 m away from point *B* at the top of the slope, the end position of the slip surface is 4 m away from point *A* at the foot of the slope, and the calculated stability factor is 1.612.

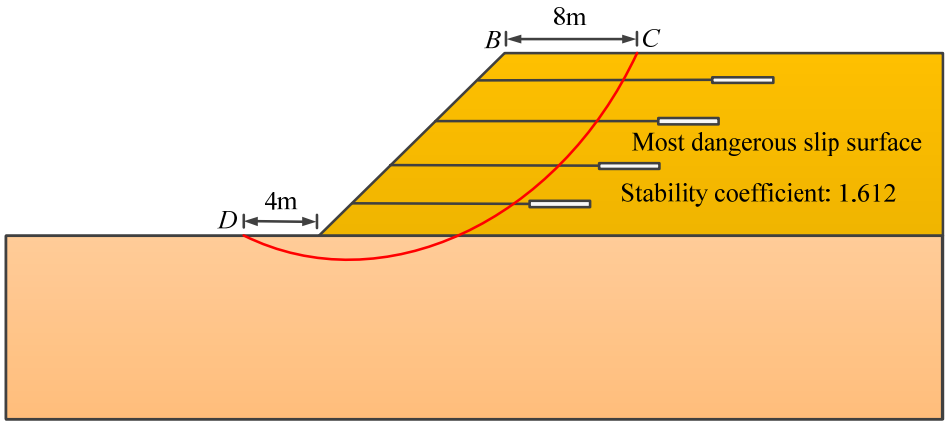


Figure 22. Example 2 calculation results of the stability of this method.

(2) Strength reduction method

The stability of example 2 is calculated with the help of PLAXIS 3D finite element software. The established three-dimensional model of the filled-slope with a slope ratio of 1:1 reinforced by the frame prestressed anchor-plates is shown in Figure 23.

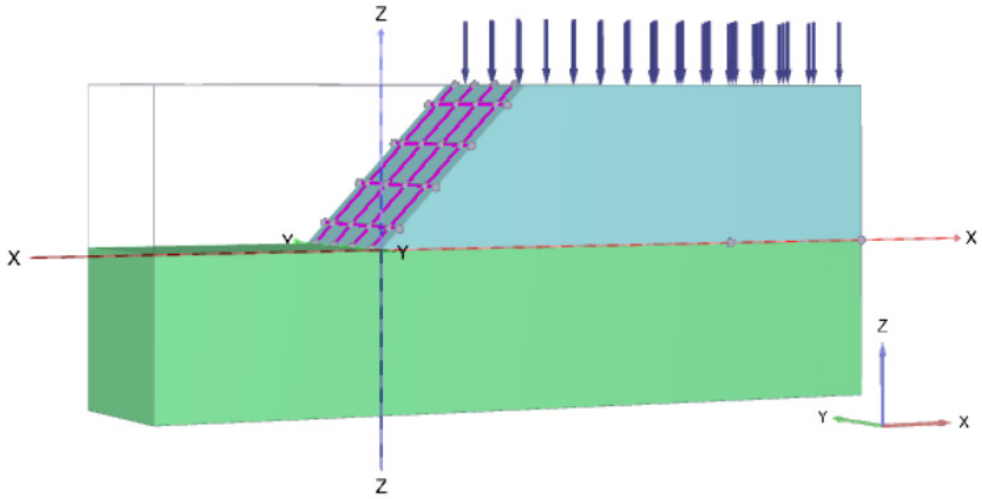


Figure 23. The 1:1 model of filled-slope reinforced by frame with prestressed anchor-plates.

Figure 24 is the total displacement increment cloud map after the calculation of the model, from which it can be clearly see that the failure mode of the slope is circular sliding failure. When the slope is damaged, the slip surface may also be far away from the toe of the slope, except for the case where the slip surface passes through the toe of the slope, and failure may occur in the deformation area of the slope. The calculated stability factor is 1.665.

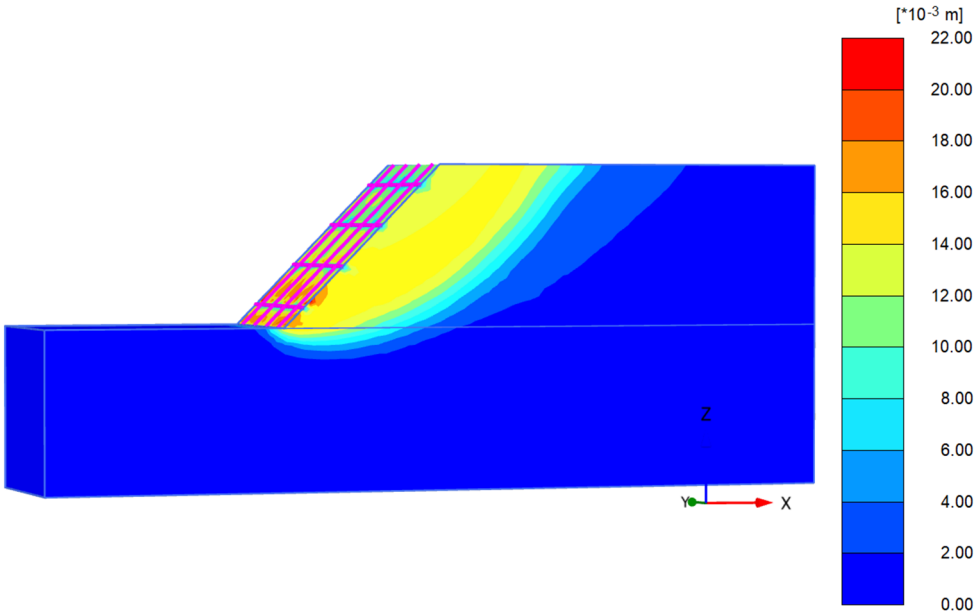


Figure 24. Total displacement increment cloud map of 1:1 model.

(3) Ultimate balance method

The Bishop method in the SLOPE module of GeoStudio 2012 finite element software is used to calculate the stability of example 2, and the specific calculation results are shown in Figure 25. From Figure 18, it can be seen that the most dangerous slip surface is far from the toe of the slope. The starting position of the slip surface is 7.5 m away from the starting point of the top of the slope, the end position of the slip surface is 4 m away from the toe of the slope, and the calculated stability factor is 1.688.

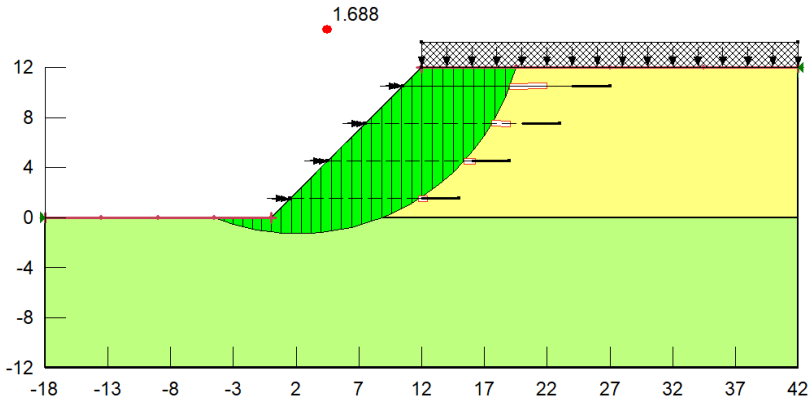


Figure 25. Example 2 calculation results of the stability of Geo.

(4) Comparative analysis

By using the above three methods to calculate the stability of example 2, it can be seen that the stability factor calculated by Geo is the largest, followed by PLAXIS 3D, and the stability factor calculated by this algorithm is the smallest. The stability factor calculated by this method respectively differs from the results simulated by Geo and PLAXIS 3D finite element software by 4.5% and 3.2%. Comparing Figure 22 with Figure 25, the shape of the most dangerous slip surface obtained by this method is similar to that obtained by Geo, both of which are far from the foot of the slope and belong to the sliding mode of midpoint circle 1.

5.3. Summary

Based the analysis of example 1 and example 2, it is concluded that although the slip surface searched by this method is not exactly the same as that searched by Geo software, the form of the slip surface is very similar, and the starting position and end position of the slip surface are similar. The stability factor calculated by this method is smaller than that calculated by the two finite element software, the specific reasons are as follows. When using PLAXIS 3D to calculate the stability factor of filled-slope reinforced by frame with prestressed anchor-plates, in addition to the reinforcement effect of the anchor-plates on the filled-slope, the frame beam also plays a certain role in reinforcing the slope, while the stability calculation method proposed in this paper only considers the effect of the anchor-plates. When using Geo to calculate the stability factor of filled-slope reinforced by a frame with prestressed anchor-plates, the software is a two-dimensional finite element software, and the anchor-plate can only be simulated as an anchor during simulation, which is different from the algorithm in this paper, so the calculated stability factor of the slope is quite different. Although the stability factor of slope calculated by this method is smaller than that calculated by finite element software, it can provide a certain safety reserve for practical engineering when designing a filled-slope reinforced by a frame with prestressed anchor-plates. Therefore, this stability calculation method of a filled-slope reinforced by a frame with prestressed anchor-plates proposed in this paper is reasonable and suitable for the case of arbitrary arc slip surface in the filled-slope reinforced by a frame with prestressed anchor-plates, and it provides some guiding values for the design of practical engineering.

6. Conclusions

In this paper, the calculation formulas of the stability factor under the four arc slip surface of a filled-slope reinforced by a frame with prestressed anchor-plates are derived by using the improved Bishop method, the corresponding search method of the most dangerous slip surface is given, and the calculation formulas of the pullout force of anchor-plates is improved. Based on two examples, the stability results calculated by the proposed algorithm are compared with those calculated by PLAXIS 3D and GeoStudio 2012 finite element software, and the following conclusions are drawn:

(1) Compared with the original calculation method of the pullout force of the anchor-plate, the pullout force of the improved anchor-plate takes into account the friction of the front and rear surface of the anchor-plate and the effect of fill cohesion in the passive earth pressure on the front end of the anchor-plate, which makes the force of the anchor-plate more complete. At the same time, it also makes the calculation theory of pullout force of anchor-plates more applicable.
(2) The stability factor of example 1 calculated by this method differs from the results simulated by PLAXIS 3D and GeoStudio 2012 finite element software by 4.6% and 7.1%, respectively, the stability factor of example 2 calculated by this method differs from the results simulated by PLAXIS3D and GeoStudio 2012 finite element software by 3.2% and 4.5%, respectively, which can meet the engineering requirements.
(3) The stability analysis method of a filled-slope reinforced by a frame with prestressed anchor-plates proposed in this paper is reasonable and suitable for the case of arbitrary arc slip surface in the filled-slope reinforced by a frame with prestressed anchor-plates, and it provides some guiding values for the design of practical engineering.

Author Contributions: Conceptualization: S.Y.; data curation: J.Z.; formal analysis: J.Z., W.L. and S.Y.; investigation: J.Z., W.L. and S.Y.; methodology: J.Z., W.L. and S.Y.; software: J.Z.; writing—original draft: J.Z. and W.L.; writing—review and editing: J.Z., W.L. and S.Y. All authors have read and agreed to the published version of the manuscript.

Funding: This research was funded by the National Natural Science Foundation of China (No. 52168050).

Institutional Review Board Statement: Not applicable.

Informed Consent Statement: The authors listed in this paper all agree to publish this paper.

Data Availability Statement: The data of simulation and theoretical calculation in the article are not freely available due to legal concerns and commercial confidentiality. Nevertheless, all the concepts and procedures are explained in the presented research and parts of the research may be available upon request.

Acknowledgments: The authors of the present work feel grateful and would like to thank Lanzhou University of Technology, GanSu CSCEC Municipal Engineering Investigation And Design Institute Co., Ltd., National Natural Science Foundation of China, for providing financial and technical support in research.

Conflicts of Interest: The authors declare that they have no conflict of interest.

References

1. Luo, X.F.; Xing, G.H.; Zhao, H. Performance of rock-soil slope reinforcement and protection effect in cutting slope construction. *Int. J. Low-Carbon Technol.* **2018**, *13*, 193–197. [CrossRef]
2. Shinoda, M.; Miyata, Y. PSO-based stability analysis of unreinforced and reinforced soil slopes using non-circular slip surface. *Acta Geotech.* **2019**, *14*, 907–919. [CrossRef]
3. Ye, S.H.; Fang, G.W.; Ma, X.R. Reliability analysis of grillage flexible slope supporting structure with anchors considering fuzzy transitional interval and fuzzy randomness of soil parameters. *Arab. J. Sci. Eng.* **2019**, *44*, 8849–8857. [CrossRef]
4. Ye, S.H.; Zhao, Z.F. Allowable displacement of slope supported by frame structure with anchors under earthquake. *Int. J. Geomech.* **2020**, *20*, 04020188. [CrossRef]
5. Nariman, K.; Mahmoud, G. Internal stability analysis of geocell-reinforced slopes subjected to seismic loading based on pseudo-static approach. *Geotext. Geomembr.* **2022**, *50*, 393–407.
6. Keskin, M.S.; Kezer, S. Stability of MSW landfill slopes reinforced with geogrids. *Appl. Sci.* **2022**, *12*, 11866. [CrossRef]
7. Varge, R.; Zlender, B.; Jelusic, P. Multiparametric analysis of a gravity retaining wall. *Appl. Sci.-Basel* **2021**, *11*, 6233. [CrossRef]
8. Varge, R.; Jelusic, P. Failure probability of an optimally designed gravity retaining wall. *ASCE-ASME J. Risk Uncertain. Eng. Syst. Part A Civ. Eng.* **2022**, *8*, 1–11. [CrossRef]
9. Sharma, S.; Saha, A.K.; Lohar, G. Optimization of weight and cost of cantilever retaining wall by a hybrid metaheuristic algorithm. *Eng. Comput. Germany* **2022**, *38*, 2897–2923. [CrossRef]
10. Konai, S.; Sengupta, A.; Deb, K. Seismic behavior of cantilever wall embedded in dry and saturated sand. *Front. Struct. Civ. Eng.* **2020**, *14*, 690–705. [CrossRef]
11. Qiu, Y.Q.; Liu, Y.; Zhang, L.J.; Wang, Z.Q. Influence of lightweight foamed concrete as backfill material on stress and deformation of buttressed earth-retaining wall. *Geofluids* **2021**, *2021*, 1–14. [CrossRef]
12. Zhao, N.Y.; Xu, Y.; Xiang, S.; Song, Y. Pressure distribution lawon vertical plate of cellular-counterfort retaining structure. *Alex. Eng. J.* **2022**, *61*, 3735–3745. [CrossRef]
13. Caputo, G.V.; Conti, R.; Viggiani, G.M.B.; Prum, C. Improved method for the seismic design of anchored steel sheet pile walls. *J. Geotech. Geoenviron.* **2021**, *147*, 1–13. [CrossRef]
14. Gazetas, G.; Garini, E.; Zafeirakos, A. Seismic analysis of tall anchored sheet-pile walls. *Soil Dyn. Earthq. Eng.* **2016**, *91*, 209–221. [CrossRef]
15. *GB 50330-2013*; Technical Code for Building Slop Engineering. China Building Industry Press: Beijing, China, 2013.
16. Ye, S.H.; Fang, G.W.; Chen, C.L.; Zhang, W.L. Numerical and monitoring analyses of new reinforcement technology of frame with prestressed anchor-plates in high filled-slope and its application. *Chin. J. Geotech. Eng.* **2018**, *40*, 57–64.
17. Zhu, Y.P.; Zhu, S.X.; Ye, S.H.; Zheng, X.J.; Zhou, Y.; Wu, Y.Q.; Li, Y.X.; Hui, C.Y.; Li, J.B.; Ma, X.R. Flexible Support System and Construction Method of Prestressed Anchor-plate for Pile-board Wall. China Patent CN10463432A, 20 May 2015.
18. Huang, A.P.; Ye, S.H. Sensitivity of high fill slope stability factors under seismic conditions. *Soil Mech. Found. Eng.* **2020**, *57*, 356–363.
19. Ye, S.H.; Fang, G.W.; Zhu, Y.P. Model Establishment and Response Analysis of Slope Reinforced by Frame with Prestressed Anchors under Seismic Considering the Prestress. *Soil Dyn. Earthq. Eng.* **2019**, *122*, 228–234. [CrossRef]
20. Bai, B.; Zhou, R.; Cai, G.Q.; Hu, W.; Yang, G.C. Coupled thermo-hydro-mechanical mechanism in view of the soil particle rearrangement of granular thermodynamics. *Comput. Geotech.* **2021**, *137*, 104272. [CrossRef]
21. Bai, B.; Yang, G.C.; Li, T.; Yang, G.S. A thermodynamic constitutive model with temperature effect based on particle rearrangement for geomaterials. *Mech. Mater.* **2019**, *139*, 103180. [CrossRef]
22. Li, Z.; Chen, S.Y.; Zhu, Y.P.; Gao, J.X. Calculation method for slope reinforced by grillage per-stressed anchor based on stability of excavation process. *Chin. J. Rock Mech. Eng.* **2014**, *33*, 2964–2970.
23. Zhu, Y.P.; Hou, X.N.; Ma, X.X.; Yang, K.B. Limit analysis of slope stability supported by framed prestressed anchor rods. *Chin. J. Geotech. Eng.* **2021**, *43*, 7–12.
24. He, L.Z.; Yuan, T.F.; Wang, X. Wall stability checking analysis on the suspended-anchor earth retaining wall of two anchor plate. *Highway Eng.* **2012**, *37*, 47–55.

25. Zhu, Y.P.; Tao, J.; Yang, X.H.; Peng, J.G.; Wu, Q. Design and numerical analyses of high-filled-slope strengthened by frame with prestressed anchor-plates. *Rock Soil Mech.* **2020**, *41*, 612–623.
26. Phung, M.V.; Nguyen, D.T.; Doan, L.T.; Nguyen, D.V.; Duong, T.V. Numerical investigation on static bending and free vibration responses of two-layer variable thickness plates with shear connectors. *IJST-T. Mech. Eng.* **2022**, *46*, 1047–1065. [CrossRef]
27. Thom, D.V.; Doan, H.D.; Minh, P.V.; Son, T.N. Finite element modeling for free vibration response of cracked stiffened FGM plates. *Vietnam J. Sci. Technol.* **2020**, *58*, 119–129. [CrossRef]
28. Liu, S.Y. *Soil Mechanics*; China Building Industry Press: Beijing, China, 2020.
29. Zhang, R.H.; Ye, S.H.; Tao, H. Stability analysis of multistage homogeneous loess slopes by improved ultimate balance method. *Rock Soil Mech.* **2021**, *42*, 813–825.
30. Zhu, D.Y.; Deng, J.H.; Tai, J.J. Theoretical verification of rigorous nature of improved Bishop method. *Chin. J. Rock Mech. Eng.* **2007**, *2007*, 455–458.
31. Pereira, T.D.; Robaina, A.D.; Peite, M.X.; Braga, F.D.A.; Rosso, R.B. Performance of analysis methods of slope stability for different geotechnical classes soil on earth dams. *Eng. Agr. Jaboticabal.* **2016**, *36*, 1027–1036. [CrossRef]
32. Sheng, K.; Hong, B.N.; Liu, X.; Shan, H. Modified Bishop method for stability analysis of weakly sloped subgrade under centrifuge model test. *Front. Struct. Civ. Eng.* **2021**, *15*, 727–741. [CrossRef]

Disclaimer/Publisher's Note: The statements, opinions and data contained in all publications are solely those of the individual author(s) and contributor(s) and not of MDPI and/or the editor(s). MDPI and/or the editor(s) disclaim responsibility for any injury to people or property resulting from any ideas, methods, instructions or products referred to in the content.